Inorganica Chimica Acta, *191* (1992) 171–177

Crystal and molecular structures of Ni(II), Pd(II) and Pt(II) complexes of methyl-2-amino-1-cyclopentenedithiocarboxylate

Eric M. Martin, Robert. D. Bereman*
Department of Chemistry, North Carolina State University, Box 8204, Raleigh, NC 27695-8204 (USA)

and Joseph Reibenspies
Department of Chemistry, Texas A&M University, College Station, TX 77843 (USA)

(Received June 18, 1991)

Abstract

Nickel(II), palladium(II) and platinum(II) complexes of methyl-2-amino-1-cyclopentenedithiocarboxylate have been synthesized and characterized crystallographically in a continued effort to examine the coordination chemistry of N_2S_2 ligand systems. The Ni(II) complex crystallizes in the tetragonal space group $P4_2/n$ with $a = 18.095(5)$, $c = 5.266(3)$ Å, $V = 1724(1)$ Å^3 and $Z = 4$. Both palladium(II) and platinum(II) compounds crystallize with a water molecule weakly bound to the two imine hydrogens of each complex, mandating formation of the *cis*-planar isomer. $Pd(C_7H_{10}NS_2)_2$ crystallizes in the triclinic centrosymmetric space group $P\bar{1}$ with $a = 7.805(3)$, $b = 9.923(4)$, $c = 12.769(4)$ Å, $\alpha = 107.62(3)$, $\beta = 101.74(3)$, $\gamma = 92.46(3)°$, $V = 917.1(6)$ Å^3 and $Z = 2$. $Pt(C_7H_{10}NS_2)_2$ also crystallizes in the triclinic space group $P\bar{1}$, with $a = 9.905(1)$, $b = 13.503(2)$, $c = 15.690(2)$ Å, $\alpha = 67.20(1)$, $\beta = 87.86(1)$, $\gamma = 71.94(1)°$, $V = 1831.0(5)$ Å^3 and $Z = 4$. A discussion of the synthesis, characterization and structural properties is presented.

Introduction

Square planar d^8 metal complexes involving sulfur coordination have attracted considerable interest because of the various structural and electronic properties brought about by strong M(II)–S bonding interactions. In light of the recent interest in the bioinorganic chemistry of nickel [1–3], there is a need for structurally characterized $Ni(II)N_2S_2$ molecules which may serve as models for the interpretation of EXAFS data.

Several X-ray absorption and diffraction studies of the active sites of nickel metalloenzymes indicate the presence of from one to four sulfur–nickel bonds [4–8]. One such investigation of carbon monoxide dehydrogenase from *Clostridium thermoaceticum* suggests that two Ni–S bonds at 2.21 Å and two Ni–N or Ni–O bonds at 1.97 Å comprise the active site [8].

In addition, unique electronic effects stem from metal–metal communication between stacks of planar molecules. Square planar dithiolenes of Ni(II) exhibit columnar stacks and, together with the Pd(II) and Pt(II) analogues, are currently under investigation as possible examples of molecular metals [9]. Other square planar d^8 metal complexes that exhibit metal–metal stacking include the Pt(II) diimine dicyanides, which have recently been reported [10].

In continuing our efforts to quantify the relationship between coordination geometries and physical properties of $M(II)N_2S_2$ systems, we have synthesized and characterized the square planar Ni(II), Pd(II) and Pt(II) complexes of methyl-2-amino-1-cyclopentenedithiocarboxylate, depicted in Fig. 1. The bis-bidentate Ni(II), Pd(II) and Pt(II) complexes of methyl-2-amino-1-cyclopentenedithiocarboxylate involve chelation through

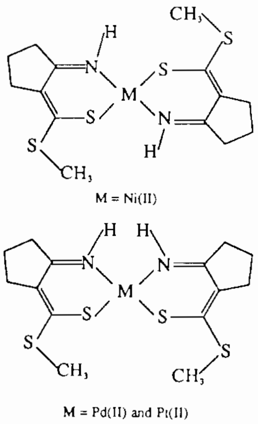

Fig. 1. Lewis structure of M(II) complexes with methyl-2-amino-1-cyclopentenedithiocarboxylate, where M(II) = Ni(II), Pd(II) and Pt(II).

---

*Author to whom correspondence should be addressed.

0020-1693/92/$5.00

a thioketonate sulfur and the lone pair on an imine nitrogen. All are square planar neutral monomers in the solid state, but the Ni(II) derivative coordinates *trans*-planar, and Pd(II) and Pt(II) derivatives in the *cis*-planar configuration due to the presence of a water molecule hydrogen bonded to the imine protons. All three complexes exhibit intense absorption in the visible region of the spectrum.

Experimental

Materials

All reagents and solvents were commercially obtained from either Fisher Scientific or Aldrich Chemicals and used without further purification. Tetraalkylammonium salts, used as supporting electrolytes, were obtained from Southwestern Analytical Chemicals, dried for 12 h at 70 °C, and used without additional recrystallization. Aldrich Gold Label solvents were used for all electrochemical studies.

Physical measurements

Electronic absorption spectra of chloroform solutions were recorded on a Cary 2300 spectrophotometer over the UV–Vis and near-IR region. The data were collected and manipulated with an Apple IIe computer.

All elemental analyses were obtained from Atlantic Microlabs, Atlanta, GA, USA, and were satisfactory.

Electrochemical properties were determined in solutions of methylene chloride and dimethylformamide, with tetraalkylammonium perchlorate salts as supporting electrolytes, and using conventional three compartment 'H' cells. A BAS CV 27 potentiostat and YEW model 3022 A4X-Y recorder were used in all cyclic voltammetry experiments. Measurements were made using a platinum disk working electrode and platinum wire auxiliary electrode, with potentials standardized against a saturated calomel electrode.

Solution ^{1}H spectra were obtained on a GE 300 MHz Omega FT-NMR spectrometer. All ^{1}H spectra were obtained using $CDCl_3$ solutions with TMS as an internal standard.

The examination and collection of data for the single crystal X-ray crystallographic study of Ni(II) $n=0$ was performed on a Nicolet R3m/V X-ray diffractometer, comprising a four-circle Eulerian cradle goniometer, sealed X-ray tube with Mo Kα radiation ($\lambda = 0.71073$ Å, operating at 55 kV and 30 MA), graphite crystal monochromator mounted with equatorial geometry, 17 cm collimator with pinhole (1.0 mm) aperture, scintillation counter with pulse height analyzer, and dedicated microprocessor (1NI CPU with μVaxII host).

Single crystal X-ray analyses of Pd(II) and Pt(II) $n=0$ were performed on a Nicolet R3m/μ diffractometer comprising a four-circle Eulerian cradle goniometer, graphite monochromator, molybdenum radiation source ($\lambda = 0.71073$ Å operating at 48 kV and 26 MA), and dedicated Data General Microeclipse microprocessor.

Synthesis

Methyl-2-amino-1-cyclopentenedithiocarboxylate was synthesized by methods previously reported [11] and isolated with sufficient purity.

Ni(II) $n=0$ was synthesized by reaction with nickel acetate in methanol [12]. A typical reaction involved dissolving 0.173 g (1.0 mmol) of $n=0$ ligand in 15 ml methanol, and adding 10 ml of methanolic nickel acetate (1.0 mmol).

The starting materials dichloro-bis-methyl(sulfinyl)-platinate(II) and palladate(II), $[M(II)(DMSO)_2Cl_2]$, were prepared by previously reported methods [13].

Palladium(II) and platinum(II) complexes were formed by addition of an ethanolic solution of $M(II)(DMSO)_2Cl_2$ (0.10 mmol) to a solution of the free ligand (0.11 mmol, 0.019 g), also dissolved in a minimal volume of absolute ethanol. The resultant orange Pd(II) and red Pt(II) precipitates were isolated by vacuum filtration, washed with ice cold absolute ethanol, then ether, and recrystallized from CH_2Cl_2. The final crop was dried at 80 °C, *in vacuo*, for 48 h in an attempt to remove any solvent molecules. All elemental analyses were satisfactory, but indicated both complexes retained one water molecule per neutral metal complex.

$C_7H_{11}NS_2$: Calc.: C, 48.55; H, 6.36; N, 8.09; S, 36.99. Found: C, 48.58; H, 6.44; N, 8.01; S, 36.91%.

$Ni(C_7H_{10}NS_2)_2$: Calc.: C, 41.48; H, 4.99; N, 6.91; S, 31.66. Found: C, 41.53; H, 4.97; N, 6.91; S, 31.49%.

$Pd(C_7H_{10}NS_2)_2xH_2O$ (**1**): Calc.: C, 35.89; H, 4.70; N, 5.98; S, 27.35. Found: C, 36.65; H, 4.76; N, 5.90; S, 27.60%.

$Pt(C_7H_{10}NS_2)_2xH_2O$ (**2**): Calc.: C, 30.16; H, 3.95; N, 5.03; S, 22.98. Found: C, 29.92; H, 3.95; N, 4.98; S, 22.83%.

Crystal data collection

$Ni(C_7H_{10}NS_2)_2$ (1)

Green needles suitable for X-ray analysis were grown by the slow evaporation of a saturated dichloromethane solution. Final unit cell parameters were calculated from the least-squares fitting of the setting angles for 25 reflections ($2\theta_{av} = 25.90$), and are collected in Table 1. Systematic absences indicated that the crystal belonged to the tetragonal space group $P4_2/n$. Inspection of axial photographs taken about each axis confirmed axis lengths and Laue symmetry. Omega scans for several intense reflections indicated good crystal quality. Data were collected for $4.0° \leqslant \theta 20 \leqslant 50.0°$ ($-21 \leqslant h \leqslant 9$, $-15 \leqslant k \leqslant 13$, $-6 \leqslant l \leqslant 3$) employing 0/20 methods. The

TABLE 1. Crystallographic data[a]

	1	2	3
Chemical formula	$C_{14}H_{20}N_2S_4Ni$	$C_{14}H_{20}N_2S_4PdxH_2O$	$C_{14}H_{20}H_2S_4PtxH_2O$
FW, AMU	403.3	469.0	557.7
Color	green	orange	red
Crystal size (mm)	0.1×0.1×0.3	0.3×0.2×0.2	0.2×0.2×0.1
Space group	$P4_2/n$	$P\bar{1}$	$P\bar{1}$
Cell dimensions			
a (Å)	18.095(5)	7.805(3)	9.905(1)
b (Å)		9.923(4)	13.503(2)
c (Å)	5.266(3)	12.769(4)	15.690(2)
α (°)		107.62(3)	67.20(1)
β (°)		101.74(3)	87.86(1)
γ (°)		92.46(3)	71.94(1)
Volume (Å^3)	1724(1)	917.1(6)	1831.0(5)
Z	4	2	4
ρ (calc.) (g/cm^3)	1.55	1.52	2.02
μ (cm^{-1})	15.9	14.2	85.0
$F(000)$ (e$^-$)	840	476	1080
Residuals (%)			
R[b]	4.50	2.15	6.66
R_w[c]	5.10	2.92	9.27
GOF[d]	2.94	1.819	4.026

[a] Radiation: Mo Kα ($\lambda = 0.71073$ Å), temperature = 296 K. [b] $R = \Sigma ||F_o| - |F_c|| / \Sigma F_o$. [c] $R_w = \{\Sigma w(\Delta F)^2 / \Sigma F_o^2\}^{0.5}$. [d] $GOF = \Sigma[w(||F_o| - |F_c||)^2/(N_o - N_v)]^{0.5}$.

quantity minimized during the least-squares procedure was $\Sigma w(F_o - F_c)^2$, where $w^{-1} = \sigma^2_F + 0.001(F)^2$. The extinction coefficient χ, where $F^* = F_c/[1 + 0.002\chi F_c^2/\sin(2\theta)]^{0.25}$, was refined to 0.00048(15) [14]. The scan range for the data collection was 1.60° plus Kα separation, with a variable scan rate of 1.50 to 15.00° min^{-1}. Three control reflections, collected every 97 reflections, showed no significant trends. Background measurements were obtained by the stationary crystal and stationary counter technique at the beginning of each scan for one-half of the total scan time.

$Pd(C_7H_{10}NS_2)_2xH_2O$ (2)

A representative orange crystal was selected, mounted on a goniometer head, and surveyed. All pertinent crystallographic data are displayed in Table 1. Cell dimensions were obtained from the least-squares fitting of 15 setting angles of the appropriate high angle reflections, and indicated the crystal belonged to the triclinic space group $P\bar{1}$. Omega scans for several intense reflections indicated good crystal quality. Data were collected for $3.0° \leq 2\theta \leq 55.0°$ ($0 \leq h \leq -17$, $-13 \leq k \leq 13$, $-17 \leq l \leq 17$). The scan range for the data collection was 2° plus dispersion, with a variable scan rate of 3.91 to 29.30° min^{-1}. Two standard reflections, collected every 98 scans, indicated no significant trends. The quantity minimized during the least-squares procedure was $\Sigma w(F_0 - F_c)^2$, where $w^{-1} = \sigma^2_F + 0.00009(F)^2$.

$Pt(C_7H_{10}NS_2)_2xH_2O$ (3)

A red crystal was selected and mounted on the goniometer for centering. Least-squares fitting of 25 setting angles of the appropriate high angle reflections produced cell dimensions indicating the crystal belonged to the triclinic space group $P\bar{1}$ (Table 1). Omega scans for several intense reflections indicated good crystal quality. Data were collected for $3.0° \leq 2\theta \leq 45.0°$ ($0 \leq h \leq 11$, $-15 \leq k \leq 15$, $-17 \leq l \leq 17$). The scan range for the data collection was 2° plus dispersion, with a variable scan rate of 3.91 to 29.30° min^{-1}. No unexpected variations were observed in check reflections taken every 98 measurements. The quantity minimized during the least-squares procedure was $\Sigma w(F_o - F_c)^2$, where $w^{-1} = \sigma^2_F + 0.00010(F)^2$. A representative set of azimuthal scans was collected and used to define pseudoellipsoids for the application of an absorption correction to the data set. Inter-layer scale factors were applied and refined routinely in order to compensate for systematic weakness along l levels.

Results

Determination and refinement of structure

$Ni(C_7H_{10}NS_2)_2$ (1)

All subsequent crystallographic calculations were performed with the SHELXTL-PLUS rev 3.4 software package [15]. Lorentz and polarization corrections were applied to 1202 reflections, and a semiempirical absorption correction was applied, based on a representative azimuthal data set. Reflection intensities were profiled using a learnt profile technique [16]. A total of 894 unique reflections ($R_{int}=0.03$*, with $|I| \geqslant 1.3\ \sigma I$, was used in further calculations. The structure was solved by direct methods using the SHELXS, SHELXTL-PLUS program [15]. Nickel was located at a special position with half occupancy. The asymmetric unit contained only half a molecule, with the second half generated by the inherent symmetry. Full-matrix least-squares anisotropic refinement for all non-hydrogen atoms (98 parameters) yielded a conventional $R=0.045$, $R_w=0.051$ and $S=2.94$ at convergence. The hydrogen atom bound to nitrogen was located in the electron density map and its coordinates added to the atom list with isotropic thermal parameter fixed at 0.08. All hydrogen atoms bound to carbon were placed in idealized positions with fixed isotropic thermal parameters. The final difference Fourier revealed the largest peak to be -0.37 e$^-$ Å^3, indicated no missing or misplaced electron density.

$Pd(C_7H_{10}NS_2)_2xH_2O$ (2) and $Pt(C_7H_{10}NS_2)_2xH_2O$ (3)

All subsequent calculations were performed with the software package SHELXTL provided by Nicolet [17]. Lorentz and polarization corrections were applied to 2737 reflections for **2**, yielding a total of 2412 unique reflections with $|I|>3\sigma I$ for use in further calculations. From a total 5342 reflections collected for **3**, 2964 unique reflections with $|I|>3\sigma I$ were used in further calculations. The heavy metal and sulfur atoms in the Pd(II) and Pt(II) structures were located by Patterson methods. The remaining non-hydrogen atoms were found by conventional difference Fourier techniques to give the appropriate trial structures. Non-hydrogen atoms were refined with anisotropic temperature factors, while all hydrogen atoms were placed in calculated positions 0.96 Å away from attached carbon nuclei and not refined. Water and imine hydrogens were not located and are absent in the final list of atomic coordinates. The structures were further refined by block diagonal least-squares refinements using SHELXTL, yielding $R=0.0215$, $R_w=0.0292$ and $GOF=1.819$ for Pd(II) $n=0$, and $R=0.0666$, $R_w=0.0927$ and $GOF=4.026$ for Pt(II) $n=0$.

Neutral atom scattering factors and anomalous scattering correction terms were taken from International Tables for X-ray Crystallography [18]. The refined structures were plotted using the SHELXTL graphics package. Atomic coordinates and anisotropic thermal parameters are given in Table 2. Selected bond distances

TABLE 2. Atomic coordinates ($\times 10^4$) and equivalent isotropic displacement parameters (Å$^2 \times 10^3$) for Ni(II), Pd(II) and Pt(II) $n=0$ complexes

	x	y	z	U_{eq} [a]
1				
Ni	10000	5000	0	34(1)
S1	8972(1)	4369(1)	−8(3)	44(1)
S2	7459(1)	4300(1)	2231(3)	43(1)
N	9700(2)	5652(2)	2539(9)	45(2)
C1	7434(3)	3635(3)	−290(10)	51(2)
C2	8330(2)	4739(3)	1975(9)	33(2)
C3	8415(3)	5336(3)	3514(10)	34(2)
C4	9087(3)	5747(3)	3760(11)	38(2)
C5	8986(3)	6338(3)	5740(11)	51(2)
C6	8185(4)	6342(4)	6327(18)	100(4)
C7	7850(3)	5647(3)	5340(11)	49(2)
2				
Pd	1216(1)	1293(1)	3961(1)	30(1)
S1	112(1)	2542(1)	2795(1)	42(1)
S2	2536(1)	3439(1)	5196(1)	40(1)
S3	−2802(1)	2152(1)	498(1)	52(1)
S4	5378(1)	4709(1)	7275(1)	53(1)
N1	38(3)	−575(3)	2873(2)	38(1)
N2	2274(3)	197(2)	4966(2)	38(1)
C1	1510(5)	4028(4)	1107(3)	66(2)
C2	1118(4)	1404(3)	1531(2)	35(1)
C3	−1451(4)	−49(3)	1196(2)	34(1)
C4	−893(4)	949(3)	1850(2)	33(1)
C5	−1537(4)	−2474(3)	1169(2)	48(1)
C6	−2726(6)	−2449(4)	94(3)	61(2)
C7	−2507(4)	−941(3)	46(2)	40(1)
C8	4685(5)	6206(3)	6847(3)	55(1)
C9	4024(4)	3196(3)	6300(2)	34(1)
C10	4347(4)	1947(3)	6532(2)	35(1)
C11	3476(4)	562(3)	5900(2)	35(1)
C12	4165(4)	−508(3)	6463(3)	41(1)
C13	5328(4)	356(4)	7596(3)	47(1)
C14	5711(4)	1854(3)	7525(3)	45(1)
Ow	8918(5)	3085(3)	6203(3)	73(1)
3				
Pt1	3638(1)	3969(1)	1108(1)	20(1)
Pt2	3659(2)	3989(1)	6152(1)	47(1)
S1	1600(18)	5059(13)	1285(5)	12(5)
S2	2347(6)	2909(5)	1068(2)	14(2)
S3	242(8)(8)	7394(6)	1438(3)	30(3)
S4	2715(10)	652(7)	1088(4)	46(4)
S5	1463(7)	5265(6)	6128(2)	11(2)
S6	2492(11)	2649(7)	6292(4)	56(4)
S7	2899(9)	382(6)	6280(3)	41(3)
S8	273(11)	7161(7)	6696(4)	52(4)
N1	4762(30)	4887(22)	1284(10)	40(10)
N2	5414(19)	2869(16)	1123(15)	13(7)
N3	4789(22)	5013(17)	6015(14)	14(7)
N4	5723(25)	2978(22)	6080(18)	36(10)
C1	−1179(42)	6837(67)	1582(42)	153(42)
C2	1936(30)	6274(21)	1354(20)	11(9)
C3	2938(34)	6600(22)	1291(17)	23(10)
C4	4410(32)	5732(24)	1265(28)	461(3)
C5	5285(28)	6548(29)	1347(22)	371(2)
C6	4655(22)	7582(18)	1379(15)	4(7)
C7	3189(26)	7520(23)	1679(16)	16(9)

(continued)

---

*$R_{int}=[\Sigma F^2-(F_{mean})^2]/[\Sigma F^2]$.

TABLE 2. (*continued*)

C8	560(39)	1221(37)	1191(40)	74(24)
C9	3262(34)	1570(27)	1172(22)	25(12)
C10	4785(31)	1291(26)	1181(23)	37(12)
C11	5738(24)	1870(22)	1124(16)	14(8)
C12	7229(42)	837(59)	1071(37)	136(38)
C13	7414(28)	79(20)	1183(20)	16(9)
C14	5930(46)	−193(29)	1209(35)	68(21)
C15	−1305(34)	6927(22)	6383(18)	21(10)
C16	1452(37)	6256(41)	6317(24)	84(19)
C17	3049(29)	6446(24)	6524(17)	22(9)
C18	4419(24)	6022(18)	6251(15)	5(7)
C19	5669(31)	6410(22)	6339(27)	39(12)
C20	4427(55)	7916(45)	5985(50)	117(31)
C21	3318(68)	7585(29)	6391(22)	127(31)
C22	1102(25)	1063(24)	6209(19)	22(10)
C23	3772(34)	1537(26)	6168(21)	28(12)
C24	5181(31)	1113(25)	6196(20)	24(11)
C25	6140(29)	1813(26)	6156(27)	43(13)
C26	7538(29)	1179(21)	6161(20)	12(9)
C27	7867(50)	−47(76)	5754(69)	227(62)
C28	5823(24)	167(18)	6202(16)	6(7)
Ow1	8142(26)	3697(23)	1008(15)	60(10)
Ow2	2016(25)	6154(26)	3737(17)	58(15)

[a]Equivalent isotropic U defined as one third of the trace of the orthogonalized U_{ij} tensor.

TABLE 3. Selected bond distances (Å) for Ni(II) and Pd(II) $n=0$ (**1** and **2**)[a]

y	**1**	**2**
M–S1	2.183(2)	2.276(1)
M–S2	2.183(2)	2.280(1)
M–N1	1.863(4)	1.996(2)
M–N2	1.863(4)	2.000(3)
S1–C2	1.770(5)	1.723(3)
C2–C3	1.359(7)	1.376(3)
C3–C4	1.431(7)	1.423(4)
N1–C4	1.294(7)	1.295(3)

[a]Ligand bond distances representative of one 'half' of the unsymmetrical Pd bis-complex.

TABLE 4. Selected bond angles (°) for Ni(II) and Pd(II) $n=0$

S1–Ni–S1A	180.0(1)	S1–Pd–S2	85.7(1)
N–Ni–NA	180.0(1)	N1–Pd–N2	86.7(1)
S1–Ni–N	94.8(1)	S1–Pd–N1	93.7(1)
S1–Ni–NA	94.8(1)	S1–Pd–N2	177.8(1)
Ni–S1–C2	112.0(2)	Pd–S1–C2	110.3(1)
S1–C2–C3	127.0(4)	S1–C2–C3	128.7(2)
C2–C3–C4	124.4(4)	C2–C3–C4	126.7(2)
C3–C4–N	127.9(5)	C3–C4–N1	127.5(2)
Ni–N–C4	133.7(4)	Pd–N1–C4	133.0(2)

and angles for compounds **1** and **2** are reported in Tables 3 and 4, respectively. See also 'Supplementary material.'

The electronic absorption spectra of the complexes in dichloromethane solution were obtained between 40.0 and 7.5 kK. Absorption maxima and molar extinction coefficients are listed in Table 5. The redox properties of the complexes were investigated by cyclic voltammetry, and are listed in Table 6. ^{1}H NMR spectral data are reported in Table 7 for **1**, **2** and **3**.

TABLE 5. Electronic absorption data[a] for the free ligand and Ni(II), Pd(II) and Pt(II) $n=0$ complexes

Complex	λ_{max} ($\pm 0.1\times 10^3$ cm^{-1}) (ϵ (M^{-1} cm^{-1}))
Ligand $n=0$	33.5(32,000), 28.5(28,000), 24.5(12,000)
Ni $n=0$	33.1(28,000), 28.1(21,000), 24.1(10,000), 22.9(15,000), 21.1(4,000), 15.7(30)
Pd $n=0$	34.4(25,000), 30.6(16,000), 24.4(6,000)
Pt $n=0$	35.3(26,000), 31.3(29,000), 29.4(sh), 21.1(7,000)

[a]All spectral data reported for CH_2Cl_2 solutions.

TABLE 6. Cyclic voltammetry responses of Ni(II), Pd(II) and Pt(II) complexes in DMF solutions (±5 mV)[a]

Complex	E_{ox}	$E_{1/2,\,red}$
Ligand $n=0$	$+1050_i$	-1750_i
Ni $n=0$	$+800_i$	$-1593(65)$
Pd $n=0$	$+950_i$	
Pt $n=0$	675_i	

[a]0.1 mM solutions with 0.1 M TEAP as supporting electrolyte. Values in parentheses represent $\Delta E_p = E_{p,c} - E_{p,a}$; i = irreversible. 200 mV/s scan rate at room temperature.

TABLE 7. ^{1}H NMR resonances (±0.05 ppm) of the free ligands and Ni(II) and Zn(II) N_2S_2 complexes

	Protons					
	1-CH_3	5-CH_2	6-CH_2	7-CH_2	NH	H_2O
Ligand N_2S_2 $n=0$	2.59	2.63	1.88	2.83	5.71, 11.25	
Ni N_2S_2 $n=0$	2.64	2.40	1.81	2.63	5.23	
Pd N_2S_2 $n=0$	2.67	2.58	1.90	2.74	6.72	1.58
Pt N_2S_2 $n=0$	2.62	2.32	1.88	2.83	6.92	1.59

Discussion

Description of structure

Atomic coordinates are given in Table 2. Selected bond distances and angles for Ni(II) and Pd(II) $n=0$ are reported in Tables 3 and 4. Figure 2(a) shows a thermal ellipsoid plot of the *trans*-Ni(II) molecule with the labelling scheme added. Figure 2(b) shows the structure of the *cis*-Pd(II) complex, which is similar to Pt(II) $n=0$. The structure of the Ni(II)N_2S_2 complex consists of well separated, neutral monomers with a planar inner coordination geometry as predicted from spectral data. The compound is planar except for the

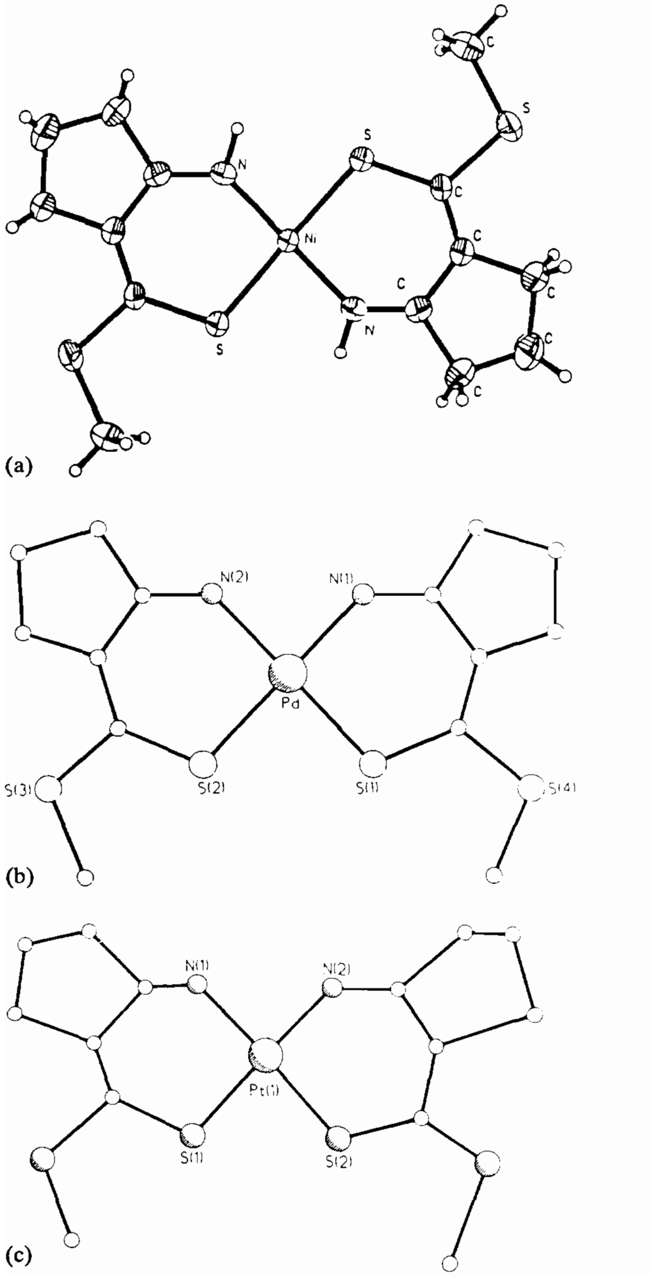

Fig. 2. Thermal ellipsoid plots of: (a) Ni(II) $n=0$ showing *trans*-configuration; (b) Pd(II) $n=0$ showing *cis*-configuration; (c) Pt(II) $n=0$ showing *cis*-configuration.

6- and 6′-CH_2 groups which lie above and below the plane, alternately. The molecules have crystallographically dictated C_2 symmetry, and fill the unit cell by stacking upon one another perpendicular to the *c* axis in an unusually ordered manner. The Ni–Ni repeat distance is the length of the *c* axis, 5.266(3) Å. Recently Wudl and co-workers published the structure of a Ni(II) dithiolate with the shortest Ni–Ni repeat distance yet observed, 4.0633(5) Å [9]. The authors note that $Ni(mnt)_2$ dianions ‘stack’ with a much longer Ni–Ni repeat distance of 8.04 Å [9]. Weak hydrogen bonding interactions exist in the *ab* plane between the imine hydrogens and non-bonded sulfur lone pairs on adjacent molecules. Ni–S and Ni–N bond lengths of 2.183(2) and 1.863(4) Å are consistent with other planar $Ni(II)N_2S_2$ structures reported [7–9]. The Ni–S distances are longer than the corresponding *cis*-planar ethylenebis(cyclopentenedithiocarboxylate) Ni–S distances (2.174(4) Å).

Although refinement of the Pt(II) $n=0$ data set resulted in the solution of the molecular structure ($R=6.76\%$), a high degree of disorder manifests itself in large standard deviations for individual bond lengths. Other possible explanations for the high R values include biases from phasing the heavy Pt(II) atoms, accuracy of the applied empirical absorption correction, and the presence of pseudosymmetry. All these problems led to unreliable positions for lighter atoms. The structure refinement for Pd(II) $n=0$ yielded very low conventional discrepancy indexes ($R=2.15\%$), and though not isomorphous with the structure of **3**, possesses roughly the same molecular structural features. Thus, the discussion of the structures of Pd(II) and Pt(II) $n=0$ will mainly concern the former. Both the palladium(II) and platinum(II) complexes of methyl-2-amino-1-cyclopentenedithiocarboxylate exist as discrete neutral monomers, exhibiting no metal–metal interaction. The favored *trans*-configuration for Pd and Pt complexes is probably prevented because of a water molecule hydrogen bonded to both imine protons.

Bond lengths within the chelating ring of the ligand indicate significant delocalization of electron density throughout a six membered ring. This quasi-aromaticity is supported by the short N–C and C–C bond lengths of 1.294(7) and 1.359(7), respectively, in the Ni(II) $n=0$ structure and lengths from 1.291–1.299 Å and 1.370–1.381 Å, respectively, for the structure of Pd(II).

Electronic absorption

The high energy regions of the electronic absorption spectra of all three complexes are dominated by absorptions giving rise to π–π^* ligand-based transitions. Broad charge transfers involving the metals dominate the visible region of the spectra. For Ni(II), maxima at 24.0, 22.7 and 21.1 kK are attributed to a combination of ligand to metal charge transfers (LMCT) involving σS–Ni(II) and πS–Ni(II) contributions. A weak d–d ligand field (LF) transition band occurs at 15.7 kK, and is common for square planar molecules with site symmetry involving a center of inversion. The *cis*-planar analogue has a lower transition energy and higher ϵ value.

The Pd(II) and Pt(II) complexes exhibit intense absorptions in the visible region of the spectrum, as well, corresponding to charge transfers from metal-based molecular orbitals into the π^* ligand-based

LUMO. A small dependence upon solvent is observed upon change from dichloromethane to dimethylformamide (DMF). LF transitions for the 4 and 5 row transition metals are expected at higher energies than their third row cogeners, and accordingly no d–d transitions are observed for the Pd(II) and Pt(II) $n=0$ complexes.

Electrochemistry

Only Ni $n=0$ undergoes reduction within the limits of ± 2000 mV of the DMF solvent system. A reversible one electron couple is observed at -1590 mV versus SCE. Reversibility is confirmed through analysis of ΔE_p, $i_{p,c}/i_{p,a}$ ratio, and scan rate dependence. A quasi-reversible oxidation is also observed ($+800$ mV), and attributed to the Ni(II)/Ni(III) redox couple. These values correspond well to the reduction potentials for the *cis*-planar Ni(II) complex, with $E_{1/2,\,\mathrm{red}} = -1540$ mV and $E_{1/2,\,\mathrm{ox}} = +750$ mV. The voltammetry of the complexes of Pd(II) and Pt(II) was more complicated. No reduction processes were observed, but complicated oxidative behavior indicates a multi-step ECE mechanism coupled to a reduction process at negative potentials. Increasingly less facile reduction processes are in accord with the increase in electronegativity of the metal. A more valuable correlation interprets more difficult reductions as a more stable environment for the divalent ion with respect to the development of the monoanionic complex. Oxidative irreversibility is indicative of decomposition of the starting complex to the disulfide.

Nuclear magnetic resonance

The diamagnetic nature of the complexes is apparent from the values of the resonances obtained. Slight broadening of the multiplets in the spectrum of Ni $n=0$ suggests a substantial amount of electron density is delocalized in the chelate rings. The spectra of the Pd(II) and Pt(II) complexes clearly reveals the peak from the water protons.

Conclusions

The *trans*-planar configuration of the $[N_2S_2]^{2-}$ complex formed with Ni(II) results from favorable stabilization of the HOMO throughout the ligand π-system. Similar coordination geometries are expected for the Pd(II) and Pt(II) structures, however, a water molecule forces *cis*-planar coordination. Delocalization within the ring structure of each chelating ring indicates that crystal packing in the proposed *trans*-Pt(II)N_2S_2 may give rise to interesting conduction properties.

Supplementary material

Hydrogen coordinates, anisotropic temperature factors, calculated and observed structure factors, and unit cell packing diagrams are available from the authors on request.

Acknowledgements

The R3m/V single-crystal X-ray diffractometer and crystallographic computing system in the Crystal and Molecular Structures Laboratory at the Department of Chemistry, Texas A&M University was purchased from funds provided by the National Science Foundation (CHE-8513273). We are indebted to help provided by Donald J. Darensbourg.

References

1 J. Lancaster (ed.), *The Bioinorganic Chemistry of Nickel*, VCH, New York, NY, USA, 1988.
2 R. P. Hausinger, *Microbiol. Rev., 51* (1987) 22.
3 R. Cammack, *Adv. Inorg. Chem., 32* (1988) 297.
4 D. V. DerVartanian, H.-J. Krüger, H. D. Peck, Jr. and J. LeGall, *Rev. Port. Quim., 27* (1975) 70.
5 S. P. J. Albracht, A. Kroger, J. W. Van der Zwaan, G. Unden, R. Bocher, H. Mell and R. D. Fontijn, *Biochim. Biophys. Acta, 874* (1986) 116.
6 P. A. Lindahl, N. Kojima, R. P. Hausinger, J. A. Fox, B. K. Teo, C. T. Walsh and W. H. Orme-Johnson, *J. Am. Chem. Soc., 106* (1984) 3062.
7 R. A. Scott, S. A. Wallin, M. Czechowski, D. V. DerVartanian, J. LeGall, H. D. Peck, Jr. and I. Moura, *J. Am. Chem. Soc., 106* (1984) 6864.
8 S. P. Cramer, M. K. Eidsness, W.-H. Pan, T. A. Morton, S. W. Ragsdale, D. V. DerVartanian, L. G. Ljundgahl and R. A. Scott, *Inorg. Chem., 26* (1987) 2477.
9 H. B. Singh, R. H. Jacobsen, K. Hinkelmann, G. Srdanov and F. Wudl, *Inorg. Chem., 28* (1989) 4221.
10 C.-M. Che, L.-Y. He, C.-K. Poon and T. C. W. Mak, *Inorg. Chem., 28* (1989) 3081.
11 P. Bordas, P. Sohar, G. Matolcsy and P. Berencsi, *J. Org. Chem., 37* (1972) 1727.
12 K. Nag and D. S. Joardar, *Inorg. Chim. Acta, 14* (1975) 433.
13 J. H. Price, A. N. Williamson, R. F. Schramm and B. B. Wayland, *Inorg. Chem., 11* (1972) 1280.
14 A. C. Larson, *Acta Crystallogr., Sect. A, 23* (1967) 604.
15 G. M. Sheldrick, *SHELXTL-PLUS*, Nicolet Analytical X-ray Instruments: Madison, WI, USA.
16 R. Diamond, *Acta Crystallogr., Sect. A, 25* (1969) 43.
17 G. M. Sheldrick, *SHELXTL*, Nicolet Analytical X-ray Instruments, Madison, WI, USA.
18 J. A. Ibers and W. C. Hamilton (eds.), *International Tables for X-Ray Crystallcgraphy*, Vol. IV, Kynoch Press, Birmingham, UK, 1974, pp. 71–102.